

Tumor Endothelin-1 contributes to macrophage infiltration and metastatic colonization of murine lungs by human cancer cells

Neveen Said ¹, Steven Smith ¹, Marta Sanchez-Carbayo ² and Dan Theodorescu ^{1*}

¹Department of Molecular Physiology, University of Virginia, Charlottesville, USA

²Spanish National Cancer Research Center (CNIO), Madrid, Spain

Type: Research Article

Key Words: bladder cancer, metastasis, endothelin, inflammation

Running Title: The Endothelin Axis in Bladder Cancer Lung Metastasis

Competing interests statement: The University of Virginia MAPS Core facility received research support from Astra Zeneca makers of ZD4054 (zibotentan) used in this manuscript. Authors declare that they have no competing financial interests in topics covered in the manuscript.

***Corresponding Author:** Dan Theodorescu: Departments of Surgery and Pharmacology and University of Colorado Comprehensive Cancer Center, Aurora, CO 80045, Tel: 303-724-7135, Fax: 303-724-3162
E-Mail: dan.theodorescu@ucdenver.edu.

Acknowledgements: This study was supported by NIH grant CA143971 to DT. The authors wish to thank Sharon Birdsall, Marya Dunlap-Brown, John Sanders and Marie Acquafondata for technical help with experiments.

SUPPLEMENTARY FIGURE LEGENDS

SUPPLEMENTARY FIGURE 1: The association between the expression ET family genes, muscle invasion and disease specific survival patient survival in human bladder cancer. Datasets were used from Sanchez-Carbayo *et al.* (*S-C et al.* N= 26 and 65, for NMI and MI disease, respectively), *GSE13507* (N= 103 and 62 for NMI and MI disease, respectively) and *UVA85* (N=36 and 24, for NMI and MI, respectively). Data for the expression of *ECE-2* (A), *ET-2* (B), *ET-3* (C), and *ET_BR* (D) were plotted using probsets identified in material and methods. Dotplots represent standardized (z-scored) logged (base 2) expression of probes comparing NMI and MI tumors and differences in distributions were tested by the Mann-Whitney U-test. Kaplan Meier curves show the association between expression of *ECE-2* (E), *ET-2* (F), *ET-3* (G), and *ET_BR* (H) expression and disease specific survival (DSS) of patients.

SUPPLEMENTARY FIGURE 2: Correlation between ET-1 expression and key inflammatory cytokines in human cancer. Scatter plots of showing the correlation of ET expression (*abscissa*) versus (A) *MMP9* (B) *MMP2*, (C) *CCL2/MCP-1*, (D) *IL-6*, and (E) *PTGS2 /Cox2* (*ordinate*, respectively) in two of the gene profiling studies (described in the material and methods). ET-1 expression is significantly correlated with the expression of each of these targets at the Spearman correlation coefficients and P-values indicated in both studies. Datapoints for the Sanchez-Carbayo *et al.* (red) and UVA-Den (blue) were logged and standardized (z-scored) study to enable facile visualization of their similar correlation patterns on the same scales, while correlation coefficients and P-values for each study are indicated in red or blue as appropriate.

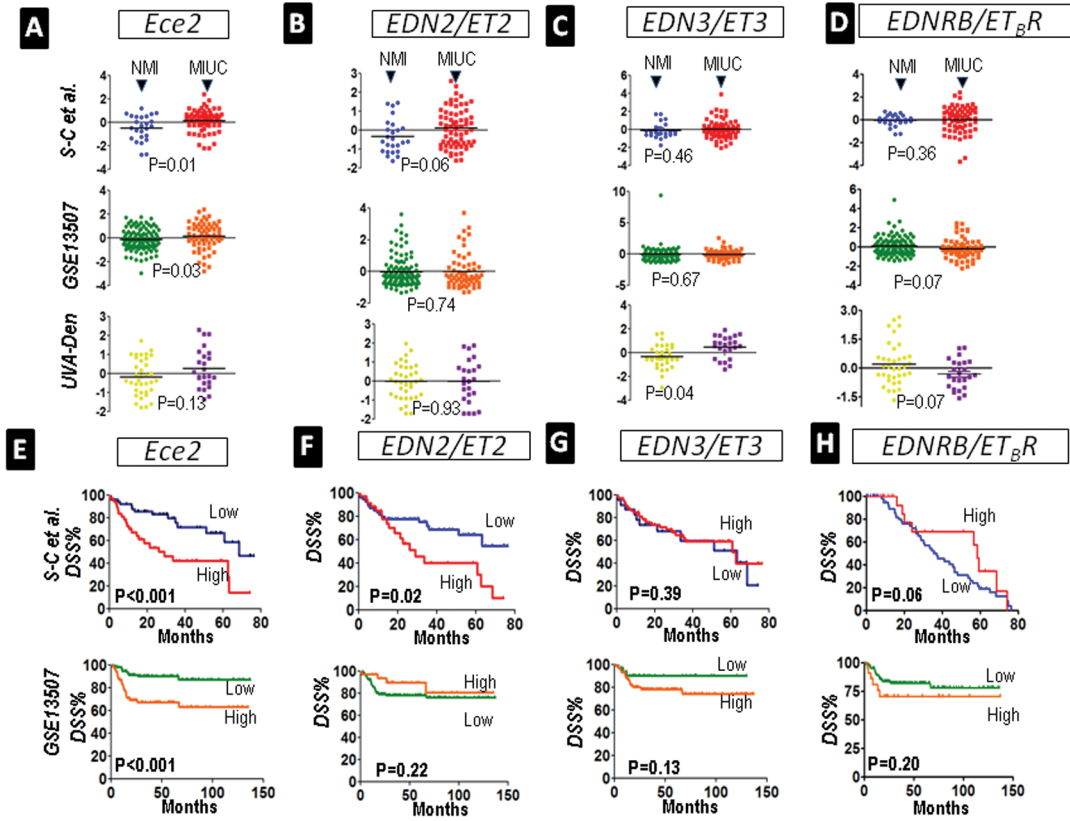
SUPPLEMENTARY FIGURE 3: Effect of co-culture of UMUC3 and U937 on cell number. UMUC3 cells (5000cells/ 1ml medium containing 2%FBS) were plated in wells of 24-well plates, and U937 (5000cells/100µl) were added on the upper well of 0.4µm inserts, either in single cell or co-culture. Each cell line was collected at 72 hours and cell number was determined by CyQuant assay.

SUPPLEMENTARY FIGURE 4: (A) Effect of ET_BR blockade on spontaneous MB49 metastasis to the lungs. Scatter plots showing the incidence and volume of lung metastases that developed 3W after subcutaneous inoculation of MB49 cells (1x10⁵/cells) in C57Bl6 mice treated or not with ET_BR blocker BQ788 before (BQ-pre) or after (BQ-post) MB49 injection. **(B)** Mac2 immunostaining of lungs harboring spontaneous MB49 metastases (100x magnification) revealed no significant difference in macrophages infiltrating the metastatic foci (in-tumor) or the surrounding lung tissue (parenchyma). **(C)** Effect of ET axis on in vitro MB49 cell proliferation. **(D)** ET-1, cytokines and Cox-2 levels in lungs 1 week after subcutaneous inoculation of MB49 cells (1x10⁵/cells) in C57Bl6 mice. *P<0.05 compared to corresponding normal lung, two-tailed Student's *t*-test.

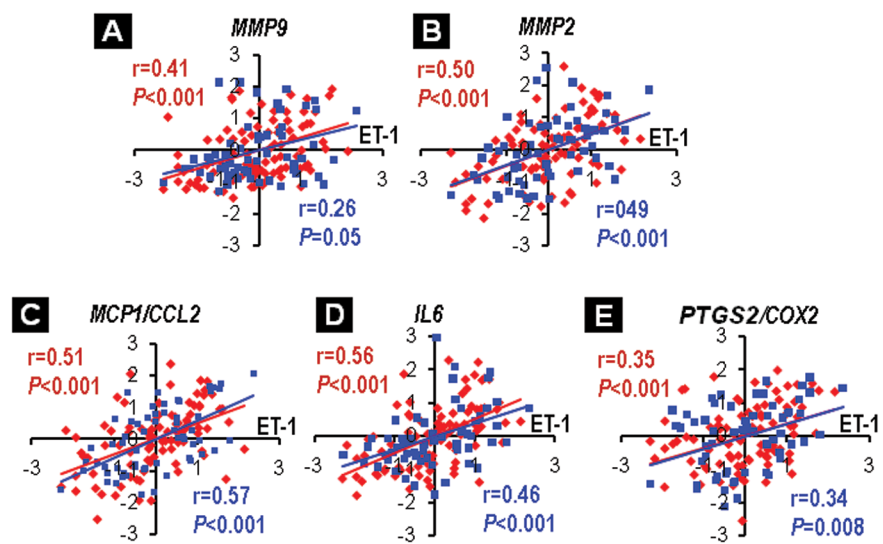
SUPPLEMENTARY FIGURE 5: (A) Expression of ET-1 axis proteins in tissue lysates. Western blots showing the expression of ECE-1, ET_AR and ET_BR proteins in lung lysates 6W after tail vein injection of control (NTsh) or UMUC3 cells depleted of ET-1 (shET-1). **(B)** Female nude mice (N=5) were injected via tail vein with 10⁶ T24 (non-metastatic) and T24T (metastatic) cells and lungs harvested at 6 weeks. Experiment was repeated with T24 stably transfected with pcDNA or pcDNA expressing ET-1 as described in methods (*inset*, western blot for ET1 and tubulin)

SUPPLEMENTARY FIGURE 6: Effect of endothelin axis manipulations on subcutaneous tumor growth. **(A)** Depletion of ET1 in UMUC3 cells by shRNA, and pharmacologic blockade of either ET_AR or ET_BR had no significant effect on the in vivo growth of UMUC3 cells after subcutaneous implantation of 1x10⁶ cells/100µl phenol red-free medium and follow up for 6 weeks. **(B)** Mac2 immunostaining of SC tumors (100x magnification) revealed no difference in macrophage infiltration. ET-1 levels **(C)**, Cox-2 activity **(D)** as well as human and murine IL-6 and MCP-1 **(E)** showed no significant difference between UMUC3-shET1 tumors and their control UMUC3-NTsh as well as between tumors from mice treated with either ZD4054 or BQ788 and their vehicle controls.

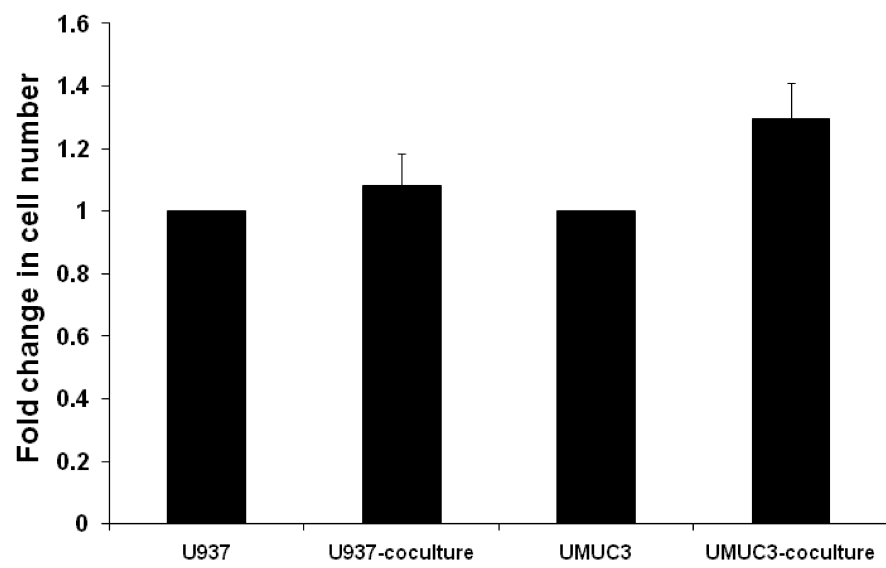
Supplementary Figure 1



Supplementary Figure 2

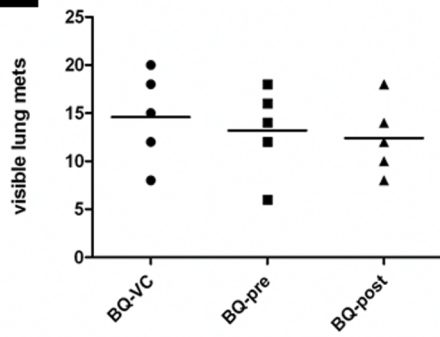


Supplementary Figure 3

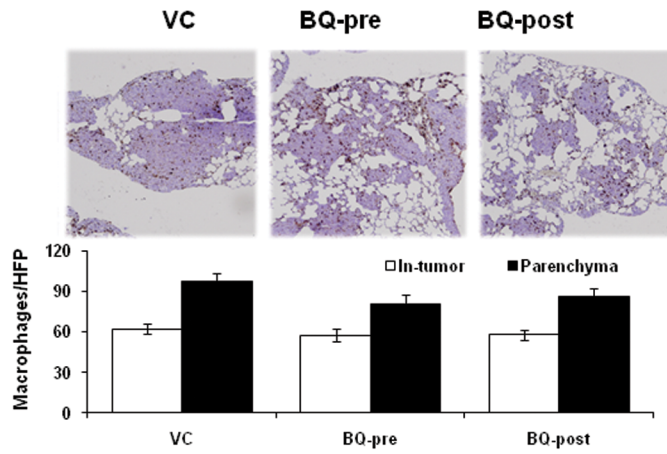


Supplementary Figure 4

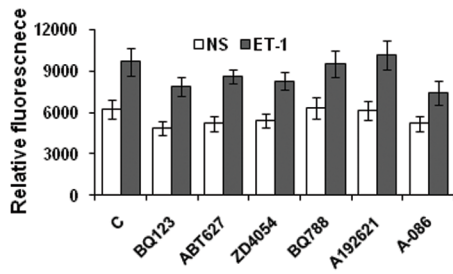
A



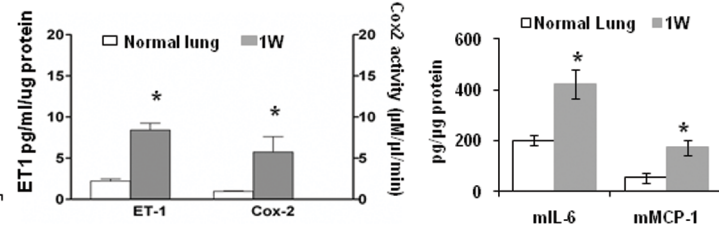
B



C



D



Supplementary Figure 6

